

# Optofluidic tunable mode-locked fiber laser using long-period grating integrated microfluidic chip

JIE WANG,<sup>1,2</sup> MIAN YAO,<sup>1,3</sup> CHENGZHI HU,<sup>1,2</sup> A. PING ZHANG,<sup>1,\*</sup>  
YONGHANG SHEN,<sup>2</sup> HWA-YAW TAM,<sup>1</sup> AND P. K. A. WAI<sup>3</sup>

<sup>1</sup>Photonics Research Center, Department of Electrical Engineering, The Hong Kong Polytechnic University, Kowloon, Hong Kong SAR, China

<sup>2</sup>State Key Laboratory of Modern Optical Instrumentation, College of Optical Science and Engineering, Zhejiang University, Hangzhou 310027, China

<sup>3</sup>Photonics Research Center, Department of Electronic and Information Engineering, The Hong Kong Polytechnic University, Kowloon, Hong Kong SAR, China

\*Corresponding author: [azhang@polyu.edu.hk](mailto:azhang@polyu.edu.hk)

Received XX Month XXXX; revised XX Month, XXXX; accepted XX Month XXXX; posted XX Month XXXX (Doc. ID XXXXX); published XX Month XXXX

**An optofluidic tunable mode-locked fiber laser using a microfluidic chip integrated with long-period grating (LPG) is presented. The microfluidic chip enables ultrafine adjustment of the liquid's refractive index (RI) and thus LPG's spectrum via tuning the mixing ratio of the microfluidic flows. With such an optofluidic spectrum-tunable filter, the central wavelength of the mode-locked laser can be tuned continuously, while the mode-locking state is steadily maintained. The mode-locked pulses are measured with pulse duration of 0.9 ps and repetition rate of 12.14 MHz, respectively. Moreover, bound solitons with variable soliton separations are experimentally demonstrated. © 2016 Optical Society of America**

**OCIS codes:** (060.3510) Lasers, fiber; (140.4050) Mode-locked lasers; (140.3600) Lasers, tunable

<http://dx.doi.org/10.1364/OL.99.099999>

Tunable mode-locked fiber lasers have received remarkable research attention because of their important applications in widespread fields, e.g. optical communications, spectroscopy and optical signal processing [1–3]. One of efficient methods to achieve tunable mode-locking is to incorporate a tunable bandpass filter (TBF) into the laser cavity [4–7]. In particular, optical fiber grating filters have drawn much attention in tunable ultrafast fiber lasers because of their compactness, low insertion loss and potential low cost [8–11]. For instance, chirped fiber Bragg gratings have been used as tunable reflectors for tunable mode-locked fiber lasers [9,10]. By using a specially designed long-period grating (LPG) W-shaped filter, our group recently demonstrated a widely tunable all-fiber mode-locked laser [11].

Tunable mode-locking is also an essential tool to investigate the underlying phenomena of mode-locked fiber lasers, including

pulse bunching [12], harmonic mode locking [13], bound solitons [14] and soliton rains [15]. Among them, bound solitons have attracted great interest because of not only the meaningful multi-soliton interaction mechanisms but also their potential applications in high-capacity fiber-optic telecommunications. However, as bound solitons are formed as a stable unit due to the balance of repulsive and attractive effects, they are vulnerable to the change of laser cavity parameters, e.g. dispersion, nonlinearity, gain and loss [16]. Therefore, there exists a demand for ultrafine TBF device to precisely adjust the overall gain of mode-locked fiber oscillator without disturbing other parameters.

One of promising approaches to achieve such ultrafine spectral tuning is the optofluidic technology, which has numerous inherent advantages including high sensitivity, reconfigurability and compactness. With the versatile microchannel networks, a microfluidic chip can be used to integrate photonic components like optical fiber gratings to develop new functional devices and applications [17–20]. In this Letter, an optofluidic tunable mode-locked fiber laser is demonstrated by using a microfluidic chip integrated with a phase-shifted LPG (PSLPG) for the first time, to the best of our knowledge. With a spiral mixer, the fluidic flows in the microfluidic chip can be sufficiently mixed and ultrafinely tune the liquid's refractive index (RI) and thus the LPG's spectrum, as shown in Fig. 1. Experimental results show that such an LPG-integrated optofluidic spectrum-tunable filter enables ultrafine tuning of the mode-locking status in the fiber oscillator.

The fabricated optofluidic chip is illustrated in Fig. 2(a), which consists of two inlets, two outlets, a spiral mixer and two throughout fiber-grating devices. To show fluidic flow networks of the chip clearly, solution with fluorescent dye Rhodamine 6G was injected before taking the photo. The microfluidic chip was fabricated in poly-dimethylsiloxane (PDMS) by using replica molding and thermal crosslinking method. The replication master was made in epoxy resin SU-8 by using an own-established optical maskless lithography platform [20]. Fig. 2(b) and (c) show the

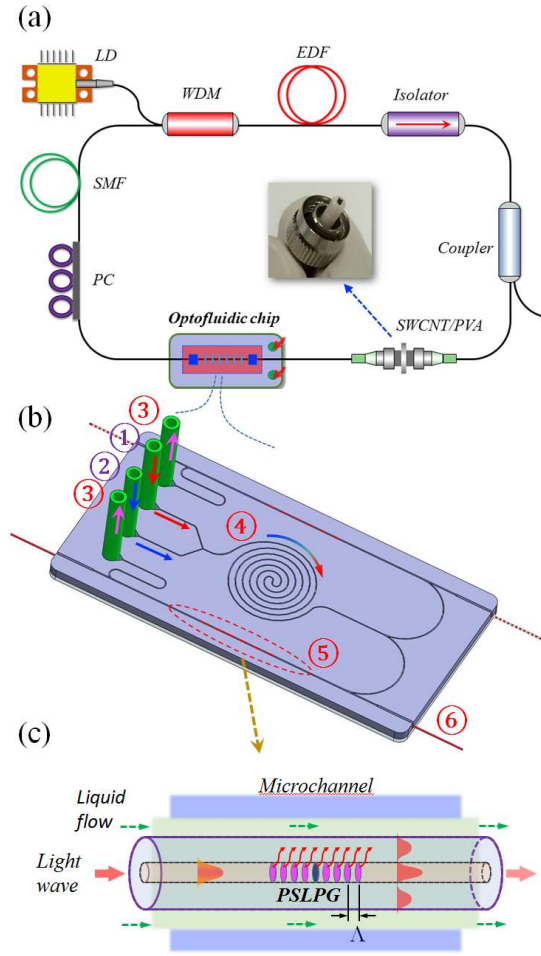


Fig. 1. Schematic diagrams of (a) the optofluidic tunable mode-locked fiber laser, (b) the LPG-integrated microfluidic chip (① and ② are the inlets, ③ is the outlet, ④ is a spiral mixer, ⑤ is the PSLPG and ⑥ is the fiber pigtail), and (c) the PSLPG filter.

spiral mixer and Y-shaped branch of the SU-8 master, which were measured by using a laser scanning confocal microscope (VK-X200, Keyence, Japan). The surface of SU-8 master is very uniform and smooth. In order to integrate optical fiber devices, the height of the SU-8 master is larger than  $150\ \mu\text{m}$ . The width of the microchannel counterpart of the spiral mixer is  $120\ \mu\text{m}$ , while the width of Y-shaped branch is  $153\ \mu\text{m}$  for interposition of optical fibers.

The PSLPG was fabricated in a photosensitive single-mode optical fiber (PS1250/1500, Fibercore Ltd.) by using a point-by-point fabrication technology [21]. Its grating period and length are  $427\ \mu\text{m}$  and  $30\ \text{mm}$ , respectively. The transmission spectrum of the PSLPG filter immersed in room-temperature de-ionized (DI) water was measured by using an optical spectrum analyzer with the resolution of  $0.02\ \text{nm}$ , as shown in Fig. 3. The central wavelength and 3-dB spectral width of its pass-band are  $1569.1\ \text{nm}$  and  $19.4\ \text{nm}$ , respectively. The extinction ratio between the pass-band and the sideband dips is around  $17\ \text{dB}$ . When the flow-rate ratio  $v$  between the calcium chloride ( $\text{CaCl}_2$ ) aqueous solution (RI

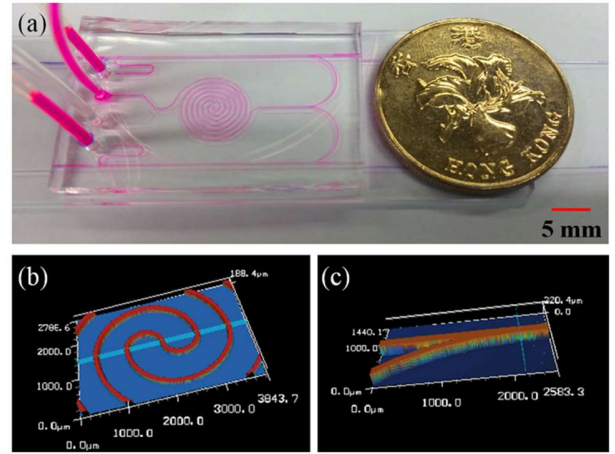


Fig. 2. (a) Photo of the LPG-integrated microfluidic chip, and the measured 3D topographic images of (b) the spiral mixer and (c) Y-shaped branch of the SU-8 master.

$\sim 1.39$ ) and DI water (RI  $\sim 1.333$ ) is adjusted by using a high-precision motorized pump, the RI of aqueous solution surrounding LPG filter can be tuned from  $1.333$  to  $1.39$ . As shown in the inset of Fig. 3, the RI change of surrounding medium will thus induce a change of the resonant wavelength of the PSLPG via the evanescent field of the corresponding optical fiber cladding mode. The central wavelength of the pass-band of PSLPG blue-shifts linearly proportional to the RI with the slope of  $93.6\ \text{nm}/\text{RIU}$ . When the microfluidic chip is driven under the injection rate of  $50\ \mu\text{L}/\text{s}$ , the spectral response time of the optofluidic tunable filter is estimated as  $0.1\ \text{s}$ .

The LPG-integrated microfluidic chip was then incorporated into a fiber oscillator to construct a tunable mode-locked fiber laser. To provide broadband gain, a  $1\text{-m}$  long erbium-doped fiber (EDF) (Liekki Er80-4/125) is forward pumped with a  $974\text{-nm}$  laser diode (LC96R74P-20R, Oclaro) via a wavelength-division

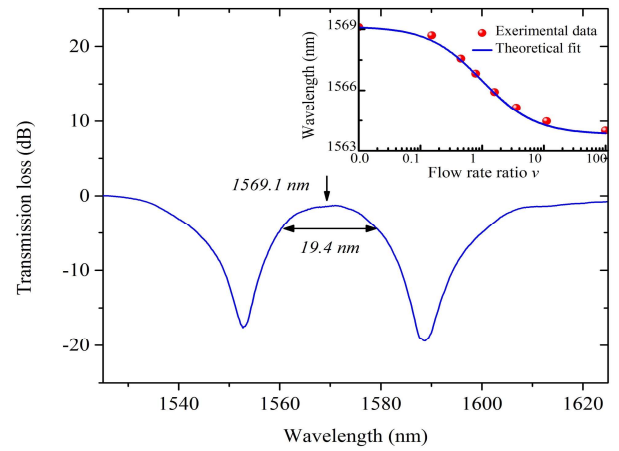


Fig. 3. Measured transmission spectrum of the PSLPG filter. The inset shows the change of its central wavelengths with respect to the flow-rate ratio.

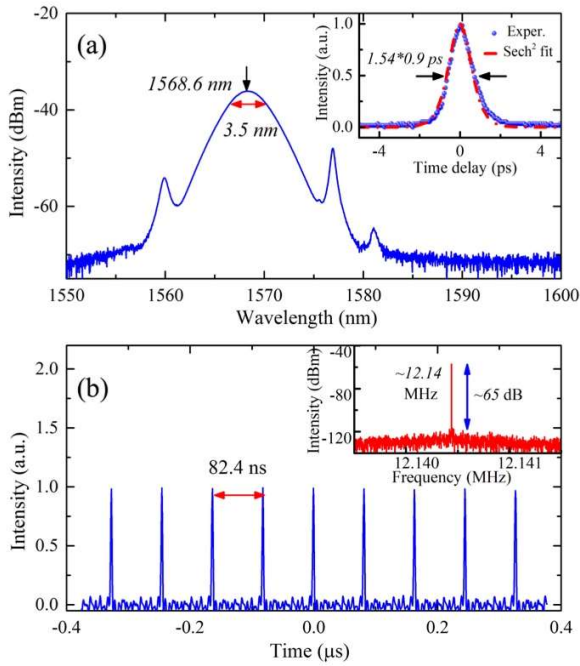


Fig. 4. (a) Typical optical spectrum and autocorrelation trace, and (b) pulse train and RF spectrum of the mode-locked fiber laser.

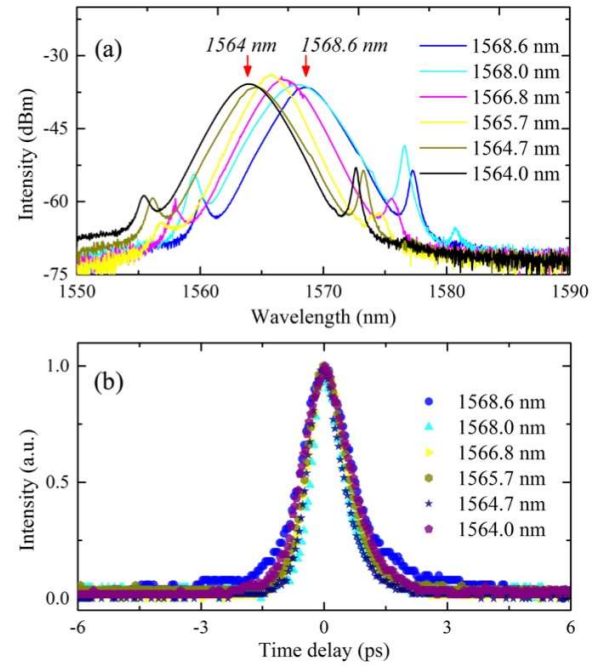


Fig. 5. (a) Optical spectra and (b) autocorrelation traces of the tunable mode-locked fiber laser at different wavelengths.

multiplexer (WDM). An optical isolator is used to force unidirectional operation of the laser. Laser is output from the 10% tap of a fiber coupler. A 5-m long single-mode fiber (SMF) with second-order dispersion of  $-22 \text{ ps}^2/\text{km}$  is inserted to form a laser cavity with net anomalous dispersion. A polarization controller (PC) is used to adjust the cavity polarization state. A saturable absorber (SA) made in SWCNT/polyvinyl alcohol (PVA) film is inserted between two FC/APC fiber connectors and acts as the mode locker. The non-saturable loss, modulation depth and saturation intensity of the SA are measured to be 95%, 5% and  $11 \text{ MW}/\text{cm}^2$ , respectively.

In the experiments, the PSLPG was utilized as an in-cavity tunable filter, whose stop bands at two sides prohibit lasing at undesirable wavelengths. At room temperature, the microfluidic chip was filled with DI water with injection rate of  $50 \text{ μL/s}$ . After pump power was increased to higher than  $43 \text{ mW}$ , self-started mode locking was obtained. Under pump power of  $50 \text{ mW}$ , typical emission spectrum of the mode-locked laser is plotted in Fig. 4(a). Kelly sidebands can be obviously observed, which indicates that the mode locking is in the anomalous dispersion regime. The central wavelength is  $1568.6 \text{ nm}$  as determined by the pass-band of PSLPG and gain profile of the laser, while the 3-dB spectral width is  $3.5 \text{ nm}$ . The mode-locked pulses are characterized by using an optical autocorrelator (Femtochrome, FR-103XL), a photodetector and an oscilloscope. With the assumption of  $\text{sech}^2$  profile, the pulse duration is evaluated to be  $0.9 \text{ ps}$ , as shown in inset of Fig. 4(a). Thus, the time-bandwidth product (TBP) is calculated to be  $0.38$ , indicating a slight chirp of the mode-locked pulses. As shown in Fig. 4(b), the pulse-to-pulse separation is  $82.4 \text{ ns}$ , corresponding to a pulse repetition rate of  $12.14 \text{ MHz}$ . The radio-frequency (RF) spectrum peak shows an SNR of  $\sim 65 \text{ dB}$ ,

indicating a stable mode locking operation state. No significant influence of laser pulses on the temperature of solutions was observed.

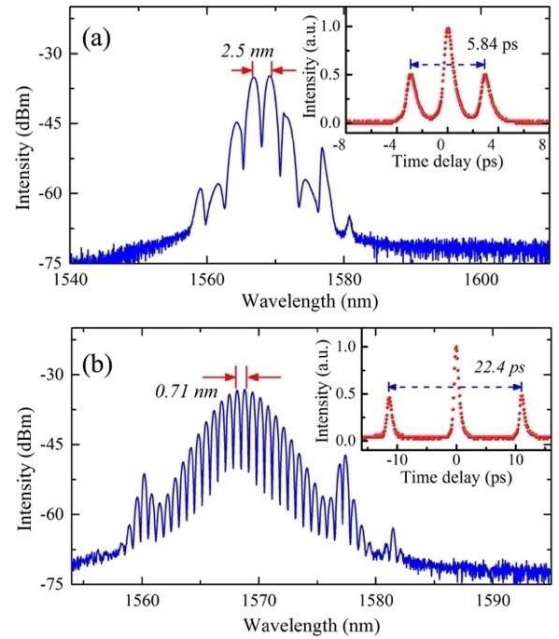


Fig. 6. Measured optical spectra and autocorrelation traces of (a) tightly and (b) loosely bounded solitons.

When the pump power is maintained at 50 mW and the PC is fixed, the emission wavelength of the mode-locked laser was tuned continuously from 1568.6 to 1564 nm by adjusting the RI from 1.333 to 1.39, as shown in Fig. 5(a). The corresponding flow-rate ratios and RIs are (0, 1.333), (0.24, 1.344), (0.68, 1.356), (1.48, 1.367), (4.18, 1.379), and (100, 1.39), respectively. The always-on Kelly sidebands mean that the mode locking state sustains during the wavelength tuning. The spectral width changes between 3.5 and 3.75 nm. The corresponding autocorrelation traces are also depicted in Fig. 5(b). The pulse duration varies from 0.74 to 1 ps. The TBP of the emitted solitons is always close to the transform limit. It is noteworthy that both the lasing threshold and the peak intensity of the laser appeared slight fluctuations at different wavelengths mainly owing to the inhomogeneous gain profile of the fiber oscillator.

Moreover, bound solitons were stably established when the PC was appropriately adjusted. Fig. 6(a) shows the optical spectrum of a tightly bounded soliton pair. In comparison to the normal spectrum of Fig. 4(a), there exists a modulation fringe on the spectrum, whose modulation period (i.e. separation between two adjacent peaks) is measured to be  $\sim 2.5$  nm. The symmetrical spectral profile indicates a  $\pi$  phase difference between the two bounded solitons [14]. As shown in the inset of Fig. 6(a), the corresponding autocorrelation trace has three peaks with intensity ratio of 1:2:1, revealing that the two bounded solitons have the same intensity and pulse duration. The soliton-to-soliton separation is measured to be 2.92 ps, which is consistent with the spectral modulation period. When the RI is changed to 1.34, another loosely bounded soliton pair was achieved, as plotted in Fig. 6(b). The spectral modulation period is shrunk to  $\sim 0.71$  nm while the soliton separation is increased to 11.2 ps. The formation of these long-distance bound solitons is attributed to the dispersive wave mediated interaction between them [22].

Compared with our previously reported LPG-based tunable mode-locking method [11], this optofluidic tunable technology has a much finer wavelength-tuning accuracy. If a microfluidic pump with the flow rate accuracy of 0.15% (e.g. using ELVEFLOW OB1-MK3, Elvesys Company) is used to control the aqueous flows of the two mixing microchannels, the resolvable RI change of the mixed aqueous solution can be calculated to be  $2.14 \times 10^{-5}$  [23]. Since the RI sensitivity of the LPG filter is 93.6 nm/RIU, one can thus estimate that the wavelength-tuning accuracy of the optofluidic technology is as high as 2.0 pm, which is significantly higher than a previously reported result using TBF [4]. On the other hand, if we assume the temperature-tuning accuracy of the packaged bulky LPG filter is 0.1°C, the typical wavelength-tuning accuracy of such a thermally-tuned LPG filter is around 72 pm [11]. Moreover, the optofluidic tunable filter owns other advantages such as high configurability. For instance, more microchannels can be fabricated to mix three or more solutions to extend tunable range or augment tunable parameters of the filter; absorptive solutions with predefined dye concentration can be used to tune its absorbance and central wavelength simultaneously.

In conclusion, a novel tunable mode-locking technology has been developed by using an LPG-integrated microfluidic chip. The optofluidic tunable filter is able to ultrafinely tune its central wavelength via precisely controlling the microfluidic flows, which has been used to continuously tune a mode-locked fiber laser from 1568.6 to 1564.0 nm. Bound solitons with variable soliton separations have also been experimentally demonstrated. Such an

optofluidic tunable mode-locking technology possesses not only ultrafine wavelength-tuning capability but also flexible configurability, which is thus promising to advance ultrafast fiber laser technology for both scientific research and industrial applications.

**Funding.** PolyU Departmental General Research Fund (G-UA4D and G-YBLJ).

## References

1. U. Keller, *Nature* **424**, 831 (2003).
2. O. Okhotnikov, A. Grudinin, M. Pessa, O. Oleg, G. Anatoly, and P. Markus, *New J. Phys.* **6**, 177 (2004).
3. V. S. Letokhov, *Nature* **316**, 325 (1985).
4. F. Wang, A. G. Rozhin, V. Scardaci, Z. Sun, F. Hennrich, I. H. White, W. I. Milne, and A. C. Ferrari, *Nat. Nanotechnol.* **3**, 738 (2008).
5. Z. Sun, D. Popa, T. Hasan, F. Torrisi, F. Wang, E. R. J. R. Kelleher, J. C. Travers, V. Nicolosi, and A. C. Ferrari, *Nano Res.* **3**, 653 (2010).
6. Y. Meng, M. Salhi, A. Niang, K. Guesmi, G. Semaan, and F. Sanchez, *Opt. Lett.* **40**, 1153 (2015).
7. Z. Yan, B. Sun, X. Li, J. Luo, P. P. Shum, X. Yu, Y. Zhang, and Q. J. Wang, *Sci. Rep.* **6**, 27245 (2016).
8. T. Erdogan, *J. Light. Technol.* **15**, 1277 (1997).
9. X. He, Z. Liu, and D. N. Wang, *Opt. Lett.* **37**, 2394 (2012).
10. J. Wang, Y. Yan, A. P. Zhang, B. Wu, Y. Shen, and H. Tam, *Opt. Express* **24**, 12618 (2016).
11. J. Wang, A. P. Zhang, Y. Shen, H. Tam, and P. K. A. Wai, *Optics Lett.* **40**, 4329 (2015).
12. D. Y. Tang, B. Zhao, L. M. Zhao, and H. Y. Tam, *Phys. Rev. E* **72**, 1 (2005).
13. A. B. Grudinin and S. Gray, *J. Opt. Soc. Am. B* **14**, 144 (1997).
14. L. Gui, X. Xiao, and C. Yang, *J. Opt. Soc. Am. B* **30**, 158 (2012).
15. S. Chouli and P. Grelu, *Opt. Express* **17**, 11776 (2009).
16. N. N. Akhmediev and A. Ankiewicz, *Phys. Rev. Lett.* **79**, 4047 (1997).
17. L. K. Chin, A. Q. Liu, J. B. Zhang, C. S. Lim, and Y. C. Soh, *Appl. Phys. Lett.* **93**, 164107 (2008).
18. K. Chao, M. Lin, and R. Yang, *Lab Chip* **13**, 3886 (2013).
19. M. I. Lapsley, S. C. S. Lin, X. Mao, and T. J. Huang, *Appl. Phys. Lett.* **95**, 2007 (2009).
20. M. Yin, B. Huang, S. Gao, A. P. Zhang, and X. Ye, *Biomed. Opt. Express* **7**, 2067 (2016).
21. A. P. Zhang, X. W. Chen, J. H. Yan, Z. G. Guan, S. He, and H. Y. Tam, *IEEE Photonics Technol. Lett.* **17**, 2559 (2005).
22. M. Olivier and M. Piché, *Opt. Express* **17**, 405 (2009).
23. C. Fang, B. Dai, R. Hong, C. Tao, Q. Wang, X. Wang, D. Zhang, and S. Zhuang, *Sci. Rep.* **5**, 15362 (2015).